Dynamic Adaptive Beam Control System Using Variable Focus Lenses for Laser Inter-Satellite Link

Kwanyong Lee, Vuong Mai, *Member, IEEE*, and Hoon Kim, *Senior Member, IEEE*

***Abstract*—One of technical challenges in laser inter-satellite link (ISL) is the mitigation of performance degradation caused by pointing errors and angle-of-arrival (AoA) fluctuations arising unavoidably from satellite movements and vibrations. In this paper, we propose the dynamic adaptive beam control (ABC) technique implementable by using variable focus lenses (VFLs) at both the transmitter and receiver. In this technique, we monitor the instantaneous pointing error and AoA fluctuation induced by satellite vibrations and then provide feedback corrections to the VFL-based ABC system. The VFLs at the transmitter and receiver adjust their focal lengths adaptively to the amount of pointing error and AoA fluctuation, respectively, to minimize the link loss. VFLs operated by electro-wetting or electromagnetic actuator are fast enough to respond to the vibrations. We design the proposed dynamic ABC system for laser ISL by using the double-lens configuration and VFLs. An exemplary system design is presented when commercially available VFLs are utilized. Our simulation study shows that the proposed dynamic ABC technique offers improved transmission performance, compared to the static and the dynamic ABC technique applied to either the transmitter or receiver.**

***Index Terms*—Adaptive beam control, free space optical communications, inter-satellite communications.**

I. Introduction

FREE-space optical (FSO) communication systems, due to the use of a narrow-divergence laser beam and an extremely high carrier frequency in the range of hundreds of terahertz, are capable of delivering high data-rate (e.g., >1 Gb/s) signals over a long distance (e.g., >1000 km). The FSO links also reduce antenna size, transponder weight, and power consumption considerably, compared to radio-frequency counterparts such as Ka-band links [1], [2]. Thus, it is anticipated that the FSO communication systems could be used for various applications including satellite and airborne links [3]–[5]. For example, the FSO communications would be used for inter-connecting numerous satellites in Starlink, a satellite internet constellation operated by SpaceX [6].

A major technical challenge of laser inter-satellite link (ISL) is the pointing, acquisition, and tracking (PAT) between the transmitter and receiver. The high orbital velocity of satellites and long transmission distances make the PAT a daunting task especially when the laser transmitter employs a narrow-divergence beam to reduce the geometric loss (i.e., the link loss induced by the size mismatch between the aperture and the beam footprint at the aperture plane). Mechanical vibrations occurring unavoidably at satellites on the move make the PAT even more challenging. This is because the vibration of the transmitter gives rise to pointing errors in FSO links, while angle-of-arrival (AoA) fluctuations occur when the receiver experiences mechanical vibrations. The optical beam misalignment caused by pointing error and AoA fluctuation reduces the optical power collected at the detector, which in turn, eventually degrades the bit-error ratio (BER) performance.

Satellites are in general equipped with highly accurate rate sensors (commonly composed of gyroscopes) for attitude control [7]. Thus, the information from those sensors can be used for correcting the optical beam misalignment caused by mechanical vibrations. Despite this feedback control, it is inevitable that laser ISLs suffer from pointing error and AoA fluctuation. This is because mechanical vibrations could be faster than the feedback correction and the angular resolution of the PAT system might not be fine enough to achieve accurate alignment.

The adaptive beam control (ABC) technique has been recently proposed and demonstrated to mitigate the adverse effect of optical beam misalignment [8]–[16]. In this technique, the beam divergence angle at the transmitter and (focused) beam radius at the detector, respectively, are adjusted adaptively to the channel conditions including the transmission distance and the amount of vibrations. This technique can be categorized into two groups according to the location where the technique is implemented. In the transmitter-side ABC technique, the divergence angle of a laser beam from the transmitter is adjusted optimally for the outage probability or average BER performance for a given pointing error. The receiver-side ABC technique controls the beam radius at the photo-detector (PD) or fiber tip at the receiver such that the optical power impinging onto the PD or fiber can be maximized for a given AoA fluctuation.

The ABC system can also be categorized into static and dynamic techniques according to the time scale of beam control. In the static ABC technique, the optimum beam divergence angle and beam radius at the detector are determined by the *statistical* information of channel conditions, such as the variance of angular deviation caused by mechanical vibrations [8]–[14]. Thus, the beam divergence angle and beam radius at the detector are controlled *slowly* in this technique. Another reason for slow control is that the static technique requires the handshake

Manuscript received April 20, 2022; revised June 14, 2022; accepted June 14, 2022. Date of publication June 17, 2022; date of current version June 30, 2022. This work was supported by the National Research Foundation of Korea funded by the Ministry of Science and ICT under Grant 2022M1A3C2069728, Space HR&D Center. *(Corresponding author: Hoon Kim.)*

The authors are with the School of Electrical Engineering, Korea Advanced Institute of Science and Technology, Daejeon, Daedeok Innopolis 34141, Korea (e-mail: haldamir3@kaist.ac.kr; vuongmai@kaist.ac.kr; hoonkim@kaist.ac.kr).

Digital Object Identifier 10.1109/JPHOT.2022.3183999

between the transmitter and receiver to exchange the statistical information. On the other hand, the dynamic ABC technique compensates for pointing errors and AoA fluctuations induced by mechanical vibrations *instantaneously* [15], [16]. In the transmitter-side dynamic ABC technique, for example, the beam divergence angle is adjusted adaptively to the instantaneous amount of transmitter vibration, whose information is provided by the rate sensors equipped in the satellite [15].

The ABC technique can be realized by using three different implementation schemes: Utilizing an optical switch to select one of multiple emitters/detectors, each having different divergence angle/ beam radius at the detector [17], changing the position of lens mechanically with respect to the position of the emitter/detector [18], and using a variable focus lens (VFL) [19], [20]. Among these schemes, the first two suffer from one or more of the following limitations: The operation speed is too slow to be used for the dynamic ABC technique; they are prone to mechanical failure; the implementation cost is very high; they have a poor beam control accuracy due to coarse granularity. In the VFL-based ABC technique, on the other hand, the focal length of VFL can be adjusted non-mechanically by changing the curvature of liquid lens. VFLs can be realized electrically by using either current-driven electromagnetic actuation or voltage-driven electrowetting [21]. Thus, the VFL-based scheme offers a low size, weight, and power (SWaP). Also, VFLs are capable of changing their focal length in the time scale of ms [22], which is fast enough to realize the dynamic ABC technique. However, due to the relatively small aperture size of VFL, it is questionable whether the VFL can be used to realize the ABC technique for laser ISL. For example, the aperture size of commercially available VFLs is smaller than 20 mm.

In this paper, we design a laser ISL featuring the transmitter- and receiver-side dynamic ABC technique using VFLs. To the best of our knowledge, this is the first study to apply the dynamic ABC technique for both the transmitter and the receiver. Thus, the laser ISL designed in this paper is capable of mitigating the adverse effects of both pointing error and AoA fluctuation caused by mechanical vibrations. We adopt the double-lens configuration for both the transmitter and receiver to overcome the limitation of small aperture size of VFL. Exemplary design values are given, taking into consideration the typical parameters of off-the-shelf VFLs available in the market. We carry out the Monte-Carlo simulation to evaluate the performance of the laser ISL designed in the paper. We show that the dynamic ABC technique outperforms the static and transmitter-only dynamic ABC techniques.

It is worth noting that there are a couple of previous works on the performance improvement and evaluation of laser ISL using the dynamic ABC technique [15], [16]. However, they employed only the transmitter-side ABC to mitigate the adverse effect of pointing error. Thus, the performance degradation induced by AoA fluctuation was not considered in these previous works. Also, they did not take into account how to realize the dynamic ABC technique. Only the optimum beam size for average BER in the presence of pointing error was derived theoretically [15].

The remainder of the paper is organized as follows. In Section II, we propose the dynamic ABC technique implementable by using VFLs at both the transmitter and receiver. In Section III, we design the proposed system using the double-lens configuration and VFLs. An exemplary set of design parameters are provided in this section. In Section IV, the performance of the laser ISL employing the designed dynamic ABC system is evaluated in the presence of pointing errors and AoA fluctuations. Finally, we conclude the paper in Section V.

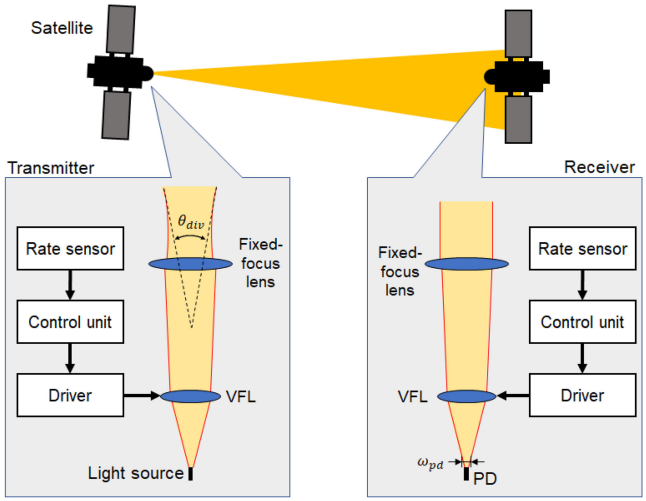

Fig. 1. Laser ISL utilizing the proposed dynamic ABC technique at the transmitter and receiver.

II. Proposed Dynamic ABC System

As explained in the Introduction, the mechanical vibrations of satellite give rise to pointing errors and AoA fluctuations in laser ISLs. The optical beam misalignment could be corrected by sensing the amount of vibrations with the aid of the rate sensors and then providing feedback on the PAT system. However, the mechanical vibrations would be too fast to be tracked by the PAT system. It was reported that the frequency components of mechanical vibration of satellites reside up to 1 kHz [23]. Due to the limited response time of the PAT system, it is very challenging to make the feedback control fast enough to track the vibrations. A coarse angular resolution of PAT would also make the PAT inaccurate in the presence of mechanical vibrations. The basic idea behind the proposed dynamic ABC technique is to mitigate the adverse effects of beam misalignment (caused by vibrations) by adjusting the beam divergence angle at the transmitter and beam radius at the detector to the amount of vibration-induced misalignment instantaneously. The beam divergence angle and beam radius at the detector are controlled non-mechanically by using VFLs. The response time of VFLs is fast enough to track the vibration-induced misalignment. For example, commercial VFLs implemented by using electromagnetic actuation exhibit a response time of a few milliseconds. It is also worth noting that the various technologies for rate sensor provide a bandwidth of $>$100 Hz [24].

The schematic diagram of the proposed dynamic ABC system is shown in Fig. 1. The system consists of the control and optical parts. The control part consists of rate sensors, a control unit,

and a VFL driver. The change in orientation of satellite induced by mechanical vibrations is first measured by the rate sensors and fed to the control unit. The control unit determines the focal length of VFL in the optical part. It should be noted that the dynamic ABC technique only requires the vibration information of the satellite where the technique is implemented, unlike the static ABC technique which needs a handshake between the satellites to exchange the statistical information of vibrations [14].

The optical part of the transmitter is composed of a light source, a VFL, and a lens. Due to the limited size of a clear aperture of VFL, we adopt the double-lens configuration. The light emitted from the light source is first sent to the VFL whose focal length is adjusted adaptively to the amount of transmitter vibration. Then, the light is fed to the lens having a fixed focal length. This lens has a larger clear aperture than the VFL. Thus, it serves to reduce the beam divergence angle tuned by the VFL. The optical part of the receiver consists of a PD, a VFL, and a lens. The PD could be replaced with an optically pre-amplified receiver or an optical coherent receiver. In this case, the light collected by the lenses is coupled into an optical fiber. The optical part of the receiver also adopts the double-lens configuration, just like that of the transmitter. Thus, a large aperture lens having a fixed focal length collects the receiving light and then sends it to the VFL. The focal length of the VFL is determined by the instantaneous amount of receiver vibration such that the optical power impinging onto the PD or fiber tip is maximized in the presence of AoA fluctuations.

III. Design of Dynamic ABC System Using Double-Lens Configuration

In this section, we design the dynamic ABC system for both the transmitter and receiver using the double-lens configuration. We focus on a laser ISL having a transmission distance longer than tens of kilometers. Thus, we consider only angular changes and neglect the displacement changes caused by satellite vibrations. This assumption has been widely used in previous studies [14].

The pointing error induced by mechanical vibrations at the transmitter leads to the beam wandering at the aperture plane of the receiver, which, in turn, increases the geometric loss. The link loss induced by the mismatch between the aperture and the beam footprint can be calculated using an area integral [25]. The fraction of optical power collected by the receiver aperture in the presence of pointing error can be expressed as

$$h_p\left(\boldsymbol{r_p}; L\right) = \int_R I_p\left(\boldsymbol{\rho_p} - \boldsymbol{r_p}; L\right) d\boldsymbol{\rho_p} \tag{1}$$

where ρ_p is the radial vector from the beam center at the receiver aperture plane, $\boldsymbol{r_p}$ is the radial vector of the misalignment of the beam center from the center of the receiver aperture due to pointing error, R is the receiver aperture area, and $I_p(; L)$ is the normalized spatial distribution of the transmitted beam intensity at transmission distance L from the transmitter. In the far-field region, we can write $\|\boldsymbol{r_p}\| = L \cdot \theta_p$ where θ_p is the pointing error. For a Gaussian beam, $I_p(\rho_p - \boldsymbol{r_p}; L)$ is given by [26]

$$I_p\left(\boldsymbol{\rho_p}; L\right) = \frac{2}{\pi L^2 \theta_{div}^2} \exp\left(-\frac{2\|\boldsymbol{\rho_p}\|^2}{L^2\theta_{div}^2}\right) \tag{2}$$

where θ_{div} is the beam divergence angle. There exists a trade-off between the geometric loss and the impact of pointing error [14]. For example, a broad divergence angle increases the geometric loss under perfect alignment, but it helps to reduce the loss in the presence of pointing error. Thus, the optimum beam divergence angle for h_p can be expressed as

$$\theta_{div,opt} = \underset{\theta_{div}}{\operatorname{argmax}}\ h_p\left(\theta_p,\ \theta_{div}\right) \tag{3}$$

Similarly, in the presence of AoA fluctuations, the fraction of the power h_a collected at the PD can be expressed as

$$h_a\left(\boldsymbol{r_a}; \omega_{pd}\right) = \int_P I_a\left(\boldsymbol{\rho_a} - \boldsymbol{r_a}; \omega_{pd}\right) d\boldsymbol{\rho_a} \tag{4}$$

where ρ_a is the radial vector from the beam center at the PD plane, $\boldsymbol{r_a}$ is the radial vector of misalignment of the beam center from the PD center due to AoA fluctuations, and P is the PD area, ω_{pd} is the beam radius at the PD, and $I_a(; \omega_d)$ is the normalized spatial distribution of the incident beam intensity into PD. For a Gaussian beam, $I_a(\rho_a - \boldsymbol{r_a}; \omega_d)$ is expressed as

$$I_a\left(\boldsymbol{\rho_a}; \omega_{pd}\right) = \frac{2}{\pi\omega_{pd}^2} \exp\left(-\frac{2\|\boldsymbol{\rho_a}\|^2}{\omega_{pd}^2}\right) \tag{5}$$

The fraction of the power, h_a, is affected by ω_{pd} and $\boldsymbol{r_p} \approx d_a \cdot \theta_a$, where d_a is the distance between the fixed-focus lens and PD and θ_a is the AoA. Then, the optimum beam radius at the PD for a given AoA can be expressed as

$$\omega_{pd,opt} = \underset{\omega_{pd}}{\operatorname{argmax}}\ h_a\left(\theta_a,\ \omega_{pd}\right) \tag{6}$$

Fig. 2(a) shows the fraction of power, h_p, as functions of the pointing error and beam divergence angle. This contour is obtained by solving (1) for a Gaussian beam. The receiver aperture radius is 50 mm and the transmission distance is 500 km. The plot also shows the optimum divergence angle for h_p. The optimum divergence increases linearly with the pointing error. This agrees well with the previously reported results in [16].

Fig. 2(b) shows the fraction of power, h_a, plotted in contour maps together with the optimum beam radius for h_a. The radius of PD is 4.5 μm and the distance between the fixed-focus lens and PD is 100 mm in this figure. When the AoA is smaller than 45 μ rad, the optimum beam radius is calculated to be smaller than the diffraction limit, which is $\sim$1.3 μm ($= 0.84\lambda f_3/D$, where λ is the wavelength, f_3 is the focal length of the fixed-focus lens at the receiver, and D represents the diameter of the fixed-focus lens). This diffraction limit comes from the beam waist of the Gaussian beam approximation having an Airy pattern, which is valid near the focal point of the circular fixed-focus lens [27]. In this case, the geometric loss occurring at the PD would be negligible since a typical size of PD is much larger than the diffraction limit. Fig. 2(b) also shows that when the AoA is larger than 100 μ rad, the optimum beam radius can be approximated to be linearly

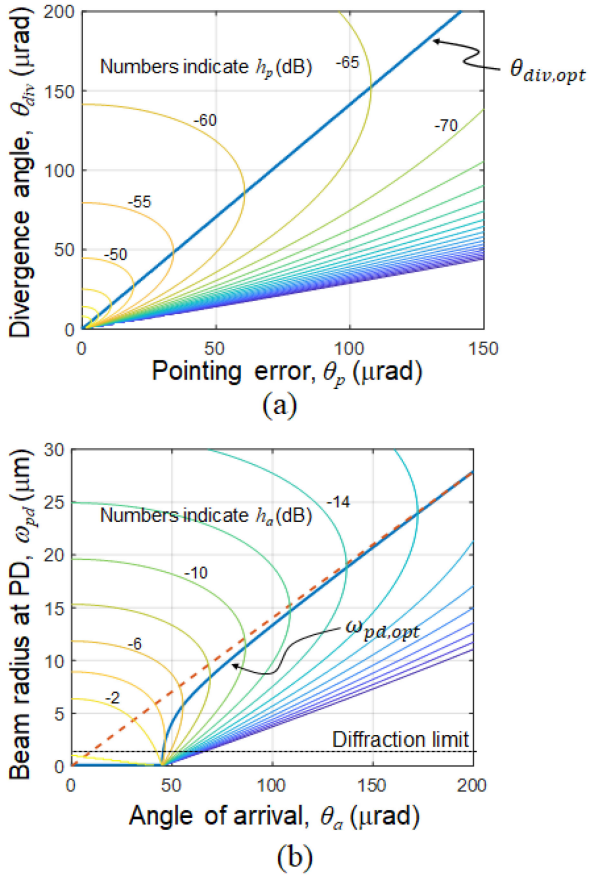

Fig. 2. (a) The fraction of power, h_p, as functions of pointing error and divergence angle (contour). The optimum divergence angle for h_p is shown in the solid line. (b) The fraction of power, h_a, as functions of AoA and beam radius at the PD (contour). The optimum beam radius and its approximation are shown in the solid and dashed lines, respectively.

proportional to AoA, which is depicted by the dashed line in the figure. This agrees very well with the result reported in [16].

We adopt the double-lens configuration to the transmitter-side optical system, as shown in Fig. 3(a). The output divergence angle of the transmitter can be obtained by using the ray transfer matrices for thin lenses and free space. The ray transfer matrix of the double-lens configuration at the transmitter is given by

$$\begin{bmatrix} A_t & B_t \\ C_t & D_t \end{bmatrix} = \begin{bmatrix} 1 & 0 \\ -1/f_2 & 1 \end{bmatrix} \begin{bmatrix} 1 & d_2 \\ 0 & 1 \end{bmatrix} \begin{bmatrix} 1 & 0 \\ -1/f_1 & 1 \end{bmatrix} \begin{bmatrix} 1 & d_1 \\ 0 & 1 \end{bmatrix} \tag{7}$$

where d_1 is the distance between the light source and VFL, d_2 is the distance between VFL and fixed-focus lens, f_1 is the focal length of VFL, and f_2 is the focal length of the fixed-focus lens. We assume that the input light to the double-lens system is delivered by an optical fiber. Thus, it has a complex parameter of $q_{in} = i\pi\omega_{0f}^2/\lambda$, where ω_{0f} is the beam waist at the fiber tip of single-mode fiber (SMF). A value of 7.8 μm is used for ω_{0f}. The complex parameter of the optical beam after the double-lens system, q_{out}, can be calculated as

$$q_{out} = \frac{A_t q_{in} + B_t}{C_t q_{in} + D_t} \tag{8}$$

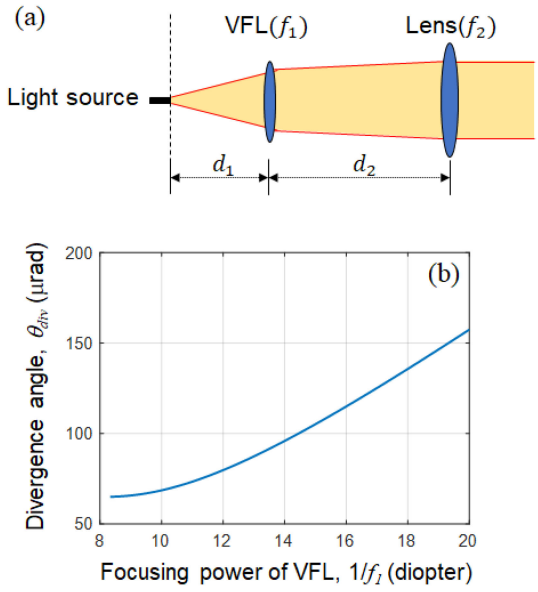

Fig. 3. (a) The double-lens configuration to implement dynamic ABC technique at the transmitter. (b) The beam divergence angle as a function of the focusing power of VFL at the transmitter.

The beam waist of the output beam from the transmitter ω_{out} can be obtained by using the following equation.

$$\frac{1}{q_{out}} = \frac{1}{R_{out}} - i\frac{\lambda}{\pi\omega_{out}^2} \tag{9}$$

Here, R_{out} represents the radius of curvature of the beam. Finally, we can obtain divergence angle θ_{div} directly from the complex parameter through $\theta_{div} = \lambda/\pi\omega_{out}$.

As a design example of the transmitter, we choose a commercial VFL having a diameter of 10 mm, operated by the electromagnetic actuator due to its fast response time and high focusing power (Optotune EL-10-30-TC) [22]. The focusing power of this VFL ranges from 8.3 to 20 diopters. The distance from the light source to the fixed-focus lens (i.e., d_1+d_2) is determined such that the beam can be collimated when the VFL has the smallest focusing power. The control range of beam divergence angle is broadened when d_1 is much smaller than d_2 since the VFL affects the beam divergence at the early stage of beam propagation. Thus, we set d_1 to be 4.8 mm, whereas d_2 is chosen to be 120 mm when f_2 is 125 mm (= 8 diopter). This parameter set gives us the minimum divergence angle close to the value achievable by a single fixed-focus lens. Fig. 3(b) shows the beam divergence angle of the designed transmitter when the focusing power of VFL varies. It shows that we can adjust the beam divergence angle of the transmitter ranging from 65 to 158 μ rad.

Fig. 4(a) shows the double-lens configuration of the receiver. We assume that a plane wave is incident on the receiver aperture, considering the long transmission distance from the transmitter. The complex parameter of the beam impinging onto the VFL is given by

$$q_{VFL} = -d_4 - i\frac{\lambda}{\pi\omega_{Airy}^2} \tag{10}$$

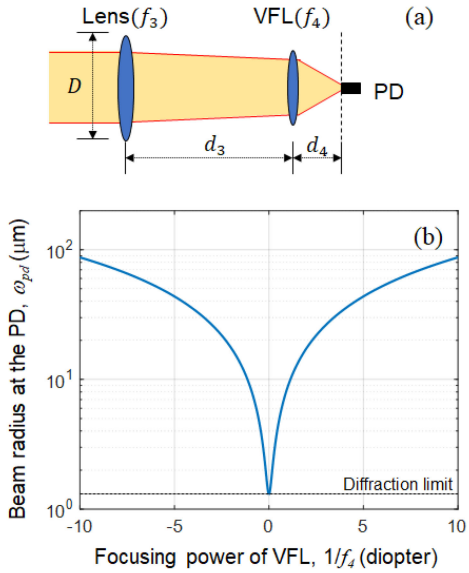

Fig. 4. (a) The double-lens configuration to implement dynamic ABC technique at the receiver. (b) The beam radius at the PD as a function of the focusing power of VFL at the receiver.

where ω_{Airy} is the approximated beam waist after the fixed-focus lens. The ray transfer matrix of the VFL and the free space between VFL and PD is given by

$$\begin{bmatrix} A_r & B_r \\ C_r & D_r \end{bmatrix} = \begin{bmatrix} 1 & d_4 \\ 0 & 1 \end{bmatrix} \begin{bmatrix} 1 & 0 \\ -1/f_4 & 1 \end{bmatrix} \tag{11}$$

where d_4 represents the distance between VFL and PD and f_4 represents the focal length of VFL. The complex parameter of the beam at the PD can be obtained as

$$q_{pd} = \frac{A_r q_{VFL} + B_r}{C_r q_{VFL} + D_r} = \left(\frac{1}{R_{pd}} - i \frac{\lambda}{\pi \omega_{pd}^2} \right)^{-1} \tag{12}$$

where ω_{pd} is the beam radius at the PD.

As a design example of the receiver, we utilize a commercial VFL having a 16-mm clear aperture (Optotune EL-16-40-TC-20D) [22]. Its focusing power ranges from -10 to 10 diopters. The diameter of the fixed-focus lens is set to be 100 mm. The focal length of the fixed-focus lens is 100 mm (= focusing power of 10 diopter). The distance between the fixed-focus lens and the PD (i.e., d_3+d_4) is chosen to be identical to the focal length of the fixed-focus lens to achieve the minimum beam radius at the PD when the focusing power of VFL is zero. Also, due to the relatively small size of VFL, we need to place VFL close to the PD. Thus, we set d_3 and d_4 to be 4.8 and 95.2 mm, respectively. Fig. 4(b) shows the beam radius at the PD as a function of the focusing power of VFL at the receiver. It shows that the beam radius changes from 1.3 to 97 μm as the focusing power of the VFL varies. The minimum beam radius in our receiver design is determined by the diffraction limit of the fixed-focus lens.

The proposed dynamic ABC technique adjusts the beam divergence angle and beam radius at the detector by changing the focusing power of VFL adaptively to the instantaneous amount of vibration. Fig. 5(a) shows the focusing power of VFL (at the transmitter) required to maximize h_p in the presence of pointing error. This result can be used to control the VFL for the pointing error measured by rate sensors. The results show that when the pointing error is smaller than 46 μ rad, the focusing power of VFL should be 8.2 diopter. This is because we have designed the transmitter such that we achieve the minimum divergence angle of 65 μ rad for this focusing power of VFL. According to (3), however, the optimum beam divergence angle for h_p is smaller than 65 μ rad when the pointing error is smaller than 46 μ rad. Thus, it is not possible for the current designed transmitter to achieve the optimum beam divergence angle in this case. For the commercial VFL we have employed in the design, we should set the focusing power to be its minimum (i.e., 8.3 dipoter), which is 0.1 diopter short of the focusing power required to achieve the minimum beam divergence angle. Despite the fact that we cannot achieve the optimum beam divergence angle in this range of small pointing errors, the adverse impact of pointing error on the system performance is not large. Thus, taking the limited range of VFL's focusing power into account, we design the transmitter such that the dynamic ABC technique at the transmitter achieves the optimum beam divergence angle for h_p when the pointing error is large. It should be noted that we can still achieve good transmission performance even though the

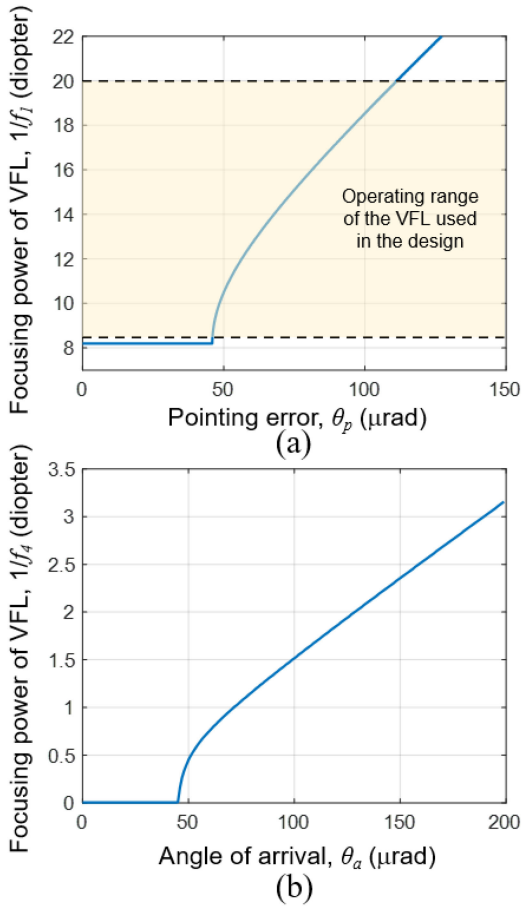

Fig. 5. Focusing power of the VFL in the designed dynamic ABC technique that maximizes the fraction of the power due to vibrations in (a) Transmitter and (b) Receiver.

optimum beam divergence angle for h_p is not achieved when the pointing error is <46 μ rad. The results show that the dynamic ABC technique mitigates the impact of pointing error up to 111 μ rad for the range of focusing power of VFL utilized in our exemplary design.

Fig. 5(b) shows the focusing power of VFL (at the receiver) required to maximize h_a in the presence of AoA fluctuation. This result can be used to control the VFL at the receiver. When the AoA fluctuation is less than 45 μ rad, the VFL should be set to zero focusing power to make the focused light fall onto the PD. As the AoA increases, however, the VFL increases ω_{pd} (by increasing the focusing power of VFL) so that a fraction of the focused light impinging onto the PD can be maximized. The designed receiver is capable of increasing ω_{pd} as large as 90 μm. Thus, the receiver provides the optimum beam radius for h_a for AoA up to 630 μ rad.

It is worth noting that the optimum θ_{div} and ω_{pd} for h_p and h_a, respectively, are governed only by the instantaneous amount of vibration measured by rate sensors. Thus, we can make lookup tables for the plots shown in Fig. 5 to control the VFLs. The use of lookup tables would make the feedback control fast, power-efficient, and easy to implement.

It is also worth mentioning that the maximum beam divergence angle could be increased by employing additional lenses in the proposed system. In this case, however, the implementation cost and SWaP also increases with the number of lenses. Also, the increased ranges of beam divergence angle would not significantly increase the transmission distance of laser ISL. This is because the maximum transmission distance is mainly limited by the minimum beam divergence angle, rather than the maximum angle, which will be shown in the next section.

IV. Simulation and Results

The performance of the proposed dynamic ABC technique is evaluated numerically by using the Monte-Carlo simulation. The pointing error and AoA fluctuations are generated as random variables having a Rayleigh distribution. Those two random variables are uncorrelated with each other. Fractions of power h_p and h_a expressed in (1) and (4), respectively, are calculated numerically for every event set of pointing error and AoA flucutation. Then, the total link loss l_{pa} is expressed in decibels as $-10\cdot\log(h_p h_a)$. On the other hand, the power margin allocated to vibration-induced link loss can be written as

$$P_m = P_l - R_s - l_i - P_{lm} \tag{13}$$

where P_l is the optical power of the laser in decibel, R_s is the receiver sensitivity, l_i is the total insertion loss of optical components including Fresnel reflections, and P_{lm} is the link margin. In this equation, the atmospheric loss is ignored due to extremely low air density in satellite orbit. Link outage occurs when $P_m < l_{pa}$. Thus, the outage probability is defined as the ratio between the number of outage cases and the number of simulated cases. The simulation is carried out 100000 times for each standard deviation of pointing error or AoA fluctuation.

The parameters used in the simulation are listed in Table I. The receiver sensitivity of -39.4 dBm corresponds to 90 photons per bit at a data rate of 10 Gb/s [1]. The maximum transmission distance is estimated from the simulation at an outage probability of 10^{-3}.

TABLE I
Parameters of the Simulation

Symbol	Quantity	Value
D	receiver aperture diameter	100 mm
P_l	optical power from laser	30 dBm
R_s	receiver sensitivity	-39.4 dBm
P_{lm}	link margin	3 dB
l_i	reflection/insertion loss	2.15 dB
D_p	PD diameter	9 μm
λ	wavelength	1550 nm
N_{sim}	number of simulations	10^5
θ_f	half divergence of a beam from the transmitter fiber end	63.3 mrad

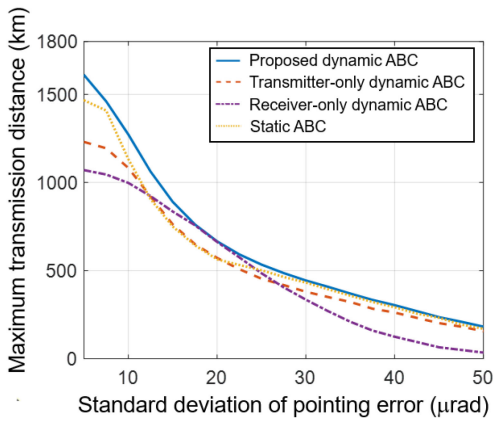

Fig. 6. The maximum transmission distances of the proposed system (solid line), the static ABC technique (dotted line), the transmitter-only dynamic ABC technique (dashed lines), and the receiver-only dynamic ABC technique (dash-dotted line) versus the standard deviations of pointing error.

Fig. 6 shows the maximum transmission distance of the proposed dynamic ABC technique as a function of standard deviation of pointing error. The standard deviation of AoA fluctuation is set to be 10 μ rad. Also shown in this figure for comparison is the maximum transmission distance for the static ABC technique. In this case, we assume that both the transmitter and receiver have the double-lens configuration, as shown in Figs. 3(a) and 4(a), respectively. Unlike the proposed dynamic ABC technique, however, the static ABC technique utilizes the statistical information about pointing errors and AoA fluctuations [14]. Thus, for given standard deviations of pointing error and AoA fluctuation, the focal lengths of VFLs do not change over time. The results show that the proposed dynamic ABC technique increases the transmission distance by 4%∼16% compared to the static technique when the standard deviation of

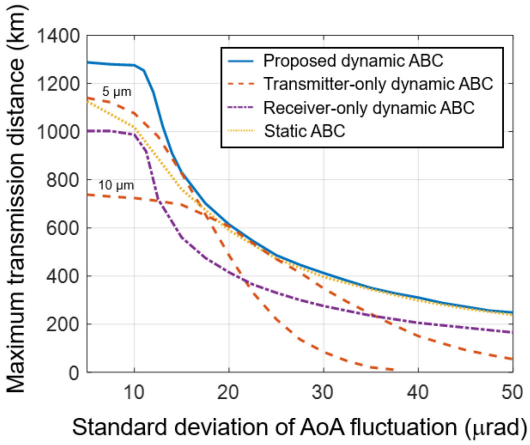

Fig. 7. The maximum transmission distances of the proposed system (solid line), the static ABC technique (dotted line), the transmitter-only dynamic ABC technique (dashed lines), and the receiver-only dynamic ABC technique (dash-dotted line) versus the standard deviations of AoA fluctuation. The numbers next to the dashed lines represent the beam radii at the PD.

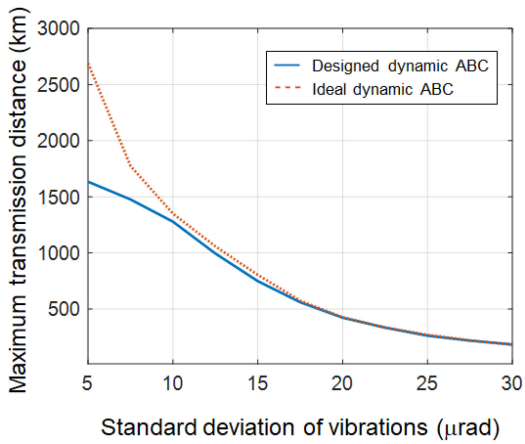

Fig. 8. The maximum transmission distance of the designed dynamic ABC system (solid line) and ideal dynamic ABC system having no limitation on beam divergence range (dotted line).

pointing error is less than 20 μ rad. However, as the pointing error exceeds 25 μ rad, the performance difference between the two techniques diminishes. This is because the probability of instantaneous pointing error being larger than 111 μ rad increases as the standard deviation of pointing error increases. As shown in Fig. 5(a), the designed transmitter is capable of mitigating the adverse effect of pointing error up to 111 μ rad. For comparison, we also plot the maximum transmission distance of the transmitter-only dynamic ABC technique. In this case, the receiver is composed of fixed-focus lenses. Thus, the beam radius at the PD is fixed to 5 μm. Since the proposed dynamic ABC technique adjusts both the beam divergence angle and beam radius at the PD adaptively to the pointing error and AoA fluctuation, respectively, the performance difference between the proposed and transmitter-only ABC technique comes from the dynamic ABC technique realized at the receiver. The results show that the proposed technique increases the transmission distance by 13%$\sim$25% in comparison with the transmitter-only dynamic ABC technique when the standard deviation of pointing error is smaller than 30 μ rad. Also shown in Fig. 6 for comparison is the maximum transmission distance of receiver-only dynamic ABC technique. In this case, the divergence angle at the transmitter is fixed to 100 μ rad. The receiver-only dynamic ABC technique underperforms the proposed dynamic ABC technique, except for the case where the standard deviation of pointing error is about 18 μ rad.

Fig. 7 shows the maximum transmission distance of the proposed dynamic ABC technique versus the standard deviation of AoA fluctuation. The standard deviation of pointing error is set to be 10 μ rad. The figure shows that we can achieve the maximum transmission distance of 1280 km by using the proposed technique when the standard deviation of AoA fluctuation is less than 10 μ rad. The maximum achievable distance decreases rapidly as the AoA fluctuation increases. This is because the AoA fluctuation makes the focused received beam fall outside of the area of PD. Although the dynamic ABC technique implemented at the receiver enlarges the beam width impinging onto the receiver, a considerable amount of power loss is incurred due to the geometric loss. Nevertheless, the results show that the proposed dynamic ABC technique outperforms the static, transmitter-only, and receiver-only dynamic ABC techniques. For example, when the standard deviation of AoA fluctuation is 20 μ rad, the proposed technique exhibits 21% longer maximum transmission distance than the transmitter-only dynamic ABC technique. The results also show that the proposed dynamic ABC technique offers better transmission performance when the AoA fluctuation is not large (e.g., standard deviation less than 20 μ rad).

In the exemplary design of the proposed dynamic ABC system, the system performance in the presence of small pointing errors is mainly limited by the focal length of the fixed-focus lens at the transmitter. This is because this focal length determines a minimum divergence angle of a beam from the transmitter. Fig. 8 shows the maximum transmission distance of the designed dynamic ABC system as a function of the standard deviations of vibrations. We assume that the standard deviation of pointing error is the same as that of AoA fluctuation in this plot. Also plotted in this figure for comparison is the maximum transmission distance of the ideal dynamic ABC system having no limitation on beam divergence range. The results show that the designed system has relatively poor performance when the standard deviation of vibrations is small. If we use a fixed-focus lens having a longer focal length, the transmitter can generate a narrower beam, which, in turn, serves to increase the maximum transmission distance when the standard deviation of vibrations is less than 10 μ rad.

V. Conclusion

We have proposed the dynamic adaptive beam control technique at both the transmitter and receiver, and designed this system implementable by using variable focus lenses. To overcome the limited ranges of beam divergence angle and focused beam radius at the detector by the relatively small size of variable focus lens, we adopt the double lens configuration at both the

transmitter and receiver. Exemplary design values are given for off-the-shelf variable focus lenses available in the market.

The proposed dynamic adaptive beam control technique is capable of mitigating the adverse effects of pointing error and angle-of-arrival fluctuation by sensing those impairments and then adjusting the focal length of variable focus lenses instantaneously at the transmitter and receiver, respectively. We evaluate the performance of the designed system through Monte-Carlo simulation. The results confirm that the proposed dynamic beam control technique improves the maximum transmission distance by a couple of tens of percent, compared to the static beam control technique. We believe that the proposed technique could be used to facilitate the beam alignment between the transmitter and receiver for laser inter-satellite links.

REFERENCES

[1] M. Toyoshima, "Trends in satellite communications and the role of optical free-space communications," *J. Opt. Netw.*, vol. 4, no. 6, pp. 300–311, May 2005.

[2] M. Toyoshima, "Recent trends in space laser communications for small satellites and constellations," *J. Lightw. Technol.*, vol. 39, no. 3, pp. 693–699, Feb. 2021.

[3] A. Trichili, M. Cox, B. Ooi, and M. Alouini, "Roadmap to free space optics," *J. Opt. Soc. Amer. B*, vol. 37, no. 11, pp. A184–A201, Nov. 2020.

[4] H. Kaushal and G. Kaddoum, "Optical communication in space: Challenges and mitigation techniques," *IEEE Commun. Surv. Tut.*, vol. 19, no. 1, pp. 57–96, Jan.–Mar. 2017.

[5] M. A. Khalighi and M. Uysal, "Survey on free space optical communication: A communication theory perspective," *IEEE Commun. Surv. Tut.*, vol. 16, no. 4, pp. 2231–2258, Oct.–Dec. 2014.

[6] Starlink, "Satellites," 2022. Accessed: Apr. 18, 2022. [Online]. Available: https://www.starlink.com/satellites

[7] M. Armenise *et al.*, "Gyroscope technologies for space applications," in *Proc. 4th Round Table Micro-Nano Technol. Space*, Noordwijk, Netherlands, 2003, pp. 1–26.

[8] V. V. Mai and H. Kim, "Adaptive beam control techniques for airborne free-space optical communication systems," *Appl. Opt.*, vol. 57, no. 26, pp. 7462–7471, Sep. 2018.

[9] H. Safi, A. Dargahi, J. Cheng, and M. Safari, "Analytical channel model and link design optimization for ground-to-HAP free-space optical communications," *J. Lightw. Technol.*, vol. 38, no. 18, pp. 5036–5047, Sep. 2020.

[10] S. Arnon, "Minimization of outage probability of WiMAX link supported by laser link between a high-altitude platform and a satellite," *J. Opt. Soc. Amer. A*, vol. 26, no. 7, pp. 1545–1552, Jul. 2009.

[11] N. Vaiopoulos, H. G. Sandalidis, and D. Varoutas, "Using a HAP network to transfer WiMAX OFDM signals: Outage probability analysis," *J. Opt. Commun. Netw.,* vol. 5, no. 7, pp. 711–721, Jul. 2013.

[12] H. G. Sandalidis, "Optimization models for misalignment fading mitigation in optical wireless links," *IEEE Commun. Lett.*, vol. 12, no. 5, pp. 395–397, May 2008.

[13] S. Arnon, "Optimization of urban optical wireless communication systems," *IEEE Trans. Wireless Commun.*, vol. 2, no. 4, pp. 626–629, Jul. 2003.

[14] V. V. Mai and H. Kim, "Beam size optimization and adaptation for high altitude airborne free-space optical communication systems," *IEEE Photon. J.*, vol. 11, no. 2, Apr. 2019, Art. no. 7902213.

[15] T. Song, Q. Wang, M. Wu, and P. Kam, "Performance of laser inter-satellite links with dynamic beam waist adjustment," *Opt. Exp.*, vol. 24, no. 11, pp. 11950–11960, May 2016.

[16] P. Do *et al.*, "Numerical and analytical approaches to dynamic beam waist optimization for LEO-to-GEO laser communication," *OSA Continuum*, vol. 3, no. 12, pp. 3508–3522, Dec. 2020.

[17] K. H. Heng, W. D. Zhong, T. H. Cheng, N. Liu, and Y. He, "Beam divergence changing mechanism for short-range inter-unmanned aerial vehicle optical communications," *Appl. Opt.*, vol. 48, no. 8, pp. 1565–1572, Mar. 2009.

[18] D. Zhou, P. G. LoPresti, and H. H. Refai, "Design analysis of a fiberbundle-based mobile free-space optical link with wavelength diversity," *Appl. Opt.*, vol. 52, no. 16, pp. 3689–3697, May 2013.

[19] V. V. Mai and H. Kim, "Non-mechanical beam steering and adaptive beam control using variable focus lenses for free-space optical communications," *J. Lightw. Technol.*, vol. 39, no. 24, pp. 7600–7608, Dec. 2021.

[20] V. V. Mai and H. Kim, "Airborne free-space optical communications for fronthaul/backhaul networks of 5G and beyond," *IEEE Future Netw. Technol. Focus*, vol. 4, no. 12, pp. 1–5, Apr. 2021.

[21] L. Chen, M. Ghilardi, J. J. C. Busfield, and F. Carpi, "Electrically tunable lenses: A review," *Front. Robot. AI*, vol. 8, Jun. 2021, Art. no. 678046. doi: 10.3389/frobt.2021.678046.

[22] Optotune, "Focus tunable lenses," 2021. Accessed: Apr. 18, 2022. [Online]. Available: https://www.optotune.com/focus-tunable-lenses

[23] M. Toyoshima, Y. Takayama, H. Kunimori, T. Jono, and S. Yamakawa, "In-orbit measurements of spacecraft microvibrations for satellite laser communication links," *Opt. Eng.*, vol. 49, no. 8, Aug. 2010, Art. no. 083604.

[24] N. El-Sheimy and A. Youssef, "Inertial sensors technologies for navigation applications: State of the art and future trends," *Satell. Navigation*, vol. 1, no. 1, pp. 1–21, 2020.

[25] A. A. Farid and S. Hranilovic, "Outage capacity optimization for free-space optical links with pointing errors," *J. Lightw. Technol.*, vol. 25, no. 7, pp. 1702–1710, Jul. 2007.

[26] B. E. A. Saleh and M. C. Teich, *Fundamentals of Photonics*. New York, NY, USA: Wiley, 1991.

[27] B. Zhang, J. Zerubia, and J. O. Marin, "Gaussian approximations of fluorescence microscope point-spread function models," *Appl. Opt.*, vol. 46, no. 10, pp. 1819–1829, Apr. 2007.